Journal of Environmental Radioactivity 167 (2017) 26–35

Contents lists available at ScienceDirect

Journal of Environmental Radioactivity

journal homepage: www.elsevier.com/locate/jenvrad

# An analysis of the radioactive contamination due to radon in a granite processing plant and its decontamination by ventilation

Pedro M. Dieguez-Elizondo [a], Tomas Gil-Lopez [b, *], Paul G. O'Donohoe [b], Juan Castejon-Navas [b], Miguel A. Galvez-Huerta [c]

[a] Public University of Navarre, Campus de Arrosadía, 31006 Pamplona, Spain
[b] Madrid Polytechnic University, Avda. Juan de Herrera, 6, 28040 Madrid, Spain
[c] Federico Santa María Technical University, Avenida España, 1680 Valparaíso, Chile

ARTICLE INFO

*Article history:*
Received 7 April 2016
Received in revised form
28 October 2016
Accepted 13 November 2016
Available online 18 November 2016

*Keywords:*
Air pollution
Human health
Radioactive contamination
Ventilation
Radon
Granite storage

ABSTRACT

This work focuses on studying concentration distribution of $^{222}$Rn radioisotope in a granite processing plant. Using Computational Fluid Dynamic Techniques (CFD), the exposure of the workers to radiation was assessed and, in order to minimise this exposure, different decontamination scenarios using ventilation were analysed. Natural ventilation showed not sufficient to maintain radon concentration below acceptable limits, so a forced ventilation was used instead. Position of the granite blocks also revealed as a determining factor in the radioactive level distribution. Thus, a correct layout of the stored material and an adequate ventilation system can guarantee free of exposure to radiation zones within the studied workshop. This leads to a drastic fall in the exposure of the workers and consequently minimises their risk of developing aggressive illness like lung cancer.



## 1. Introduction

The three main decay chains observed in nature (called thorium, uranium and actinium series) contain radon gaseous element ($^{220}$Rn, $^{222}$Rn and $^{219}$Rn isotopes respectively). The half-live of these isotopes are 55.6 s, 3.82 d and 3.96 s, respectively, then, $^{222}$Rn isotope is the only one that has a long enough life to be able to permeate through the rock into the air (Ferrero, 2013).

It is well known that inhalation of radon and their decay products constitute the largest fraction (52%) of radiation dose received by humans from natural background radiation (UNSCEAR, 2006, 2000a, 2000b). Indoor radon exposure has been linked to lung cancer cases in several studies (BEIR, 1999; Castren et al., 1985; Chen et al., 2010; WHO, 2009).). According to the United States Environmental Protection Agency, radon is the number one cause of lung cancer among non-smokers (ATSDR, 1990; U.S. EPA, 2003). This serious associated illness, the difficulty in detecting the gas (it is colourless, odourless and tasteless) and its zero chemical reaction make radon a highly dangerous gas (El-Hussein, 2005; Higgy et al., 2000).

There are many rocks that emit natural radiation, particularly those of metamorphic origin such as granite which contain all the radioisotopes of the mentioned half-life chains (Righi and Bruzzi, 2006; Taylor and McLennan, 1985). Therefore, a confined space containing metamorphic rock such as granite -material widely used in construction for ornamental purposes-poses a serious potential danger in the long term for human beings (Chao et al., 1997a; Gil-Lopez et al., 2013a; Stoulos et al., 2003).

Given the seriousness of exposing workers to high levels of radon concentration, there are extensive regulations (European Commission, 2001; WHO, 2009), as well as indications on the repercussions of these levels of concentration on workers' health (IAEA, 2006). These regulations are mandatory at international (ICRP, 2009; UNSCEAR, 2006; WHO, 2007), European (European

*Abbreviations: Ac*, concentration of radon, Bq·m$^{-3}$; *M*, molecular mass of $^{222}$Rn, 222.01752 g/mol; *m*, mass of $^{222}$Rn present in 1 m$^3$ of contaminated air, pg; *N*, number of $^{222}$Rn atoms in the whole volume of the plant; $N_{av}$, Avogadro number, 0.60225·10$^{24}$ atoms/mol; *R*, ventilation rate in the plant, h$^{-1}$; *t*, time, s; *T*, $^{222}$Rn escaped from granite to the surrounding air, 26.85 atoms of $^{222}$Rn /(s·kg); $T_{1/2}$, half-life period of $^{222}$Rn, 3.82 days; $V_g$, volume of granite, 200 m$^3$; $V_r$, plant volume, 15 640 m$^3$; $\lambda$, decay constant of $^{222}$Rn, 2.10014·10$^{-6}$ s$^{-1}$; $\rho$, granite density, 2880 kg m$^{-3}$.

* Corresponding author.
*E-mail address:* tomas.gill@upm.es (T. Gil-Lopez).

http://dx.doi.org/10.1016/j.jenvrad.2016.11.016
0265-931X/

Commission, 2001, 1999a, 1999b, 1997) and Spanish levels (RD 1439, 2010). In most cases, the permissible levels of radon in places of work, residence and leisure are set according to the term of exposure.

Studies for understanding radon release and for developing systems to control it are crucial for exposure control research. The information on radon emission processes, as well as on how it is transported and distributed in the environment, is essential for determining the permissible exposure limits to radon sources and radiation dose calculation due to the impact of radon on indoor air quality and consequent inhalation hazard. On the other hand, development of various mitigation techniques is crucial for controlling the dose due to radon and its progeny (Cavallo et al., 1996).

In confined volumes, radon has a nonuniform concentration distribution that depends on the flow field established in the volume, which is in turn governed by the airflow rate, the geometry of the volume, the inlet and outlet positions, etc. (Agarwal et al., 2016).

The radon distribution and its state of mixing inside the volume, is best simulated using software based on Computational Fluid Dynamics (CFD). Some works exist wherein CFD has been used to study radon distribution in rooms and dwellings (Agarwal et al., 2014; Urosevic et al., 2008; With and Jong, 2011; Zhuo et al., 2001).

Traditionally, indoor radon levels have been measured by passive methods using dosimeters and active methods using electronic devices, for example, continuous radon monitors. Some mathematical models are also developed to estimate the indoor radon concentration (Jelle et al., 2011; Stoulos et al., 2003). In recent times, CFD has taken outstanding position for simulation of indoor radon problems. CFD solves the governing fluid equations and provides spatial and temporal field solution of variables such as pressure, temperature and concentrations. It also provides velocity flow field and the dispersion pattern of indoor pollutant (Chauhan et al., 2014; Gil-Lopez et al., 2014, 2013b). Ability of commercially available CFD software to simulate a wide range of geometrical and environmental conditions is one of its striking advantages over other existing tools. Many CFD based studies have been carried out to model the entry of soil gas radon into buildings (Andersen, 2001; Loureiro, 1987; Wang and Ward, 2002, 2000, 1997). But limited CFD based studies have been performed to investigate indoor radon dispersion (Akbari et al., 2013; Urosevic et al., 2008; Zhuo et al., 2001).

This research uses a CFD model to analyse the concentration of radon in a granite processing plant and the performance of different alternatives of ventilation used to keep radon concentration level below the permissible levels.

## 2. Material and method

The purpose of this work is to measure the concentration of radon ($^{222}$Rn isotope) in the air that may be potentially inhaled by the workers in a granite handling plant. In the research, only the radon emitted by the granite blocks has been considered. Atoms emitted from the walls, floor or other construction material have not been taken into account.

For the purpose of determining the mass of $^{222}$Rn and its distribution throughout the building, the characteristics of the plant and the material properties (volume, morphology, density and exhalation rate of the granite) have to be previously addressed.

A granite handling and processing plant was chosen as granite is a rock that is in wide commercial use and has a high rate of $^{222}$Rn atoms escaped to the air (Sakoda et al., 2011; Chen et al., 2010).

### 2.1. Characteristics of the plant

The activity in the studied plant is the production of granite slabs out of $2 \times 5 \times 2$ m granite blocks.

The plant comprises two closed workshops and a central space designed to store granite blocks. In the right hand workshop the granite blocks are cut and in the left hand one, they are transformed into slabs of thicknesses between 2 and 5 cm.

Each of the workshops has a rectangular shape of $80 \times 22$ m and is 9 m high. In one of the shorter sides there is an $8 \times 8$ m door (64 m$^2$), protected by a strip curtain with an air permeability of 80 m$^3$/h·m$^2$ for a pressure difference of 100 Pa. The top part of the building has a longitudinal ventilation opening of $80 \times 0.8$ m (64 m$^2$).

The study focuses on one of the workshops since both have the same shape and dimensions.

### 2.2. Material characteristics

In order to find the contamination produced by the radioactive decay products of radon inside the workshops, the dimensions and characteristics of the granite blocks are first analysed (IAEA, 2003; Taylor and McLennan, 1985).

The granite that is handled in the plant is of the Rojo Sayago variety. It was chemically analysed by an ICP − MS (Inductively Coupled Plasma Mass Spectrometry), by the Chemical Analysis Service of Salamanca University to define its elements and traces. The granite's chemical composition is set out separately depending on whether its components are higher than 1‰ (Table 1) or lower (Table 2). The concentration of the major components is expressed as a percentage in weight of the corresponding oxides of which the sum of the percentages must be approximately 100.

The most relevant chemical element found in the analysis is $^{238}$U, the first radioisotope in the natural chain of radioactive decay. The remainder of the radioisotopes in the series, like $^{226}$Ra (direct predecessor of $^{222}$Rn) can be calculated from the secular radioactive equilibrium, considering that all radioisotopes have equal activity.

### 2.3. Adopted methodology

The decontamination of the radon radioactive decay products has some characteristics that make it markedly different from other types of decontamination. The radon passes into the air from the rock slowly and gradually. It cannot be detected by smell or colour. Being a noble gas it has a zero chemical reaction, which means that techniques based on chemical capture or combination with reagents are not viable. The only feasible technique for decontaminating is to dilute the gas with air, that is to say, using a ventilation-extraction technique (Chao et al., 1997b; NCRP, 1997).

One of the conditioning factors of the problem is that an extremely small amount of radon present in the air can be highly dangerous for health.

**Table 1**
Main components of the granite.

| Components | Quantity (%) |
|---|---|
| $Al_2O_3$ | 14.32 |
| CaO | 1.06 |
| $Fe_2O_3$ | 2.05 |
| $K_2O$ | 7.18 |
| MgO | 1.48 |
| MnO | 0.04 |
| $Na_2O$ | 6.05 |
| $P_2O_5$ | 0.31 |
| $SiO_2$ | 66.14 |
| $TiO_2$ | 0.32 |
| Volatile | 2.43 |

**Table 2**
Minor components of the granite.

| Components | Concentration (ppm) |
|---|---|
| Ba | 402 |
| Be | 237 |
| Co | 27 |
| Cr | 30 |
| Li | 25 |
| Nb | 17 |
| Ni | 25 |
| Pb | 65 |
| Sr | 154 |
| Th | 21.2 |
| U | 4.3 |
| V | 36 |
| Zn | 97 |
| As, Cd, Cu, S, Se | 0 |

$$Ac = \lambda \cdot (m/M) \cdot N_{av} \qquad (1)$$

For 300 $Bq \cdot m^{-3}$ of radiation in the contaminated air, which is considered the maximum limit by the health authorities, the amount of radon is $5.27 \cdot 10^{-14}$ g in 1 $m^3$ of air. To put it another way, a single atom of radon for approximately every $3.76 \cdot 10^{17}$ atoms of oxygen or nitrogen in the air makes this air dangerous for health.

Such small amounts are not easily detectable by sensors. The measurements are not instantaneous but require a relatively long period of integration. This circumstance means that prevention is the only solution as it is impossible to know instantaneously the dose of radiation being received. It is also impossible to carry out experiments to produce a radon radiation map of a specific contaminated space.

For the aforegoing reasons, Computational Fluid Dynamic Techniques (CFD) are the most plausible way to perform an analysis of the radiation protection required in confined spaces where radon is generated.

### 2.4. The radon-air mixing process

The interactions or acting forces in this process are: 1) Inertial forces (ventilation and extraction), 2) Dispersion forces of $^{222}Rn$ in the air, and 3) Buoyancy forces due to gravity.

The dominant forces in the radon-air mix phenomenon will be the inertial forces (due to the ventilation-extraction system). It is also obvious that the phenomenon can be controlled by modifying the amount of air introduced/extracted.

The dispersion forces will tend to cause the radon atoms to be uniformly spread throughout the volume of the closed space. They have much less effect than the inertial forces but tend to be important in the absence of ventilation. The dispersion coefficient of $^{222}Rn$ in air is 0.1 $cm^2\ s^{-1}$, at 298 K (NCRP, 1997).

The amount of $^{222}Rn$ escaped from the samples to the surrounding air is very small. Specifically, for Rojo-Sayago granite it is 0.203 atoms disintegrated per hour —or 26.85 atoms of $^{222}Rn$ per second— for each kilogram of granite. In the case analysed in this research, taking the density and volume of the stored granite blocks, it is of the order of $5.7 \cdot 10^{-15}$ g $s^{-1}$ for the entire workshop. These small amounts do not lead to any appreciable variations in density even though the density of $^{222}Rn$ is almost eight times that of air. This means that the buoyancy forces are negligible for the most part of the plant except in the volume immediately next to the emitting surfaces of the granite, where the concentration gradient is somewhat higher.

Radon and air mixing is, as far as its chemical and physical properties are concerned, air with so low a percentage of radon that it does not affect either its aerodynamics or its chemical properties, although it certainly affects its radiological properties. Thus, a CFD study of a radon-air mixing is essentially a CFD study of air, in which a small amount of atoms of radon is dragged. It is in this field, the performance of ventilation systems, where CFD studies have strongly proved their reliability (Gil-Lopez et al., 2013a, 2013b).

### 2.5. Analysed scenarios

The consideration of perfect dilution of radon in the air of the workshop or, otherwise, considering the existence of spatial gradients is a determining factor in the mathematical complexity of the problem, and therefore is decisive in the use of one or other calculation tool.

Assuming that the dilution is perfect, the concentration of radon is uniform throughout the plant. The phenomenon is governed by a simple differential equation of a single independent variable, the time, which is easily integrable.

If spatial gradients are taken into account, the variation in the concentration of radon with the position, the mass conservation, movement quantity and dispersion equations must be solved simultaneously. To address this problem, ANSYS-CFX V15.0 simulation software was used for this work.

ANSYS-CFX is a well-known finite elements software. With this tool, the geometry of the granite processing plant has been discretized in a mesh of approximately $3.2 \cdot 10^6$ elements (with slight variations between the symmetric and asymmetric arrangement hypothesis). This implies an average size per element of about 4.9 L that guarantees robust enough results. The k-ε turbulence model has been used in the forced ventilation simulations. On the contrary, laminar flow has been considered when natural ventilation has been simulated. The code simultaneously solves the Navier-Stokes equations and the diffusion equation, after 4000 iterations. Energy equation has been neglected, since the process of diffusion of $^{222}Rn$ is considered isothermal, at 298 K constant temperature.

Set out below are the analysed scenarios. In the ideal scenario of uniform concentration, perfect dilution or zero spatial concentration gradients, the theoretical study is performed with and without air renewal. If spatial gradients are considered, the simulations are presented with natural ventilation and with forced ventilation for airflow rates of 80, 120, 160 and 200 $m^3/(m^2 \cdot h)$. In all the simulations, two different distributions of the granite blocks, asymmetric and symmetric, were taken into account. Two studies and ten simulations were thus carried out.

#### 2.5.1. Uniform concentration scenario

The emission of $^{222}Rn$ atoms into the air is constant, since it depends on the mass of granite and *T*, atoms of $^{222}Rn$ escaped from granite to the surrounding air. The removal of $^{222}Rn$ atoms depends on two factors: its radioactive decay and *R*. the ventilation air change rate. The rate of change with time of $^{222}Rn$ atoms, are determined by Eq. (2).

$$dN/dt = T \cdot \rho \cdot V_g - (\lambda + R)N \qquad (2)$$

Solution to this differential equation, being $N_0$ the number of $^{222}Rn$ atoms in the initial time instant t = 0, is expressed by Eq (3).

$$N = \left[(T \cdot \rho \cdot V_g)/(\lambda + R)\right]\{1 - \exp[-(\lambda + R)t]\} + N_0 \exp[-(\lambda + R)t] \qquad (3)$$

*λN,* in disintegrated atoms per unit time and unit volume of contaminated air, being $Ac_0$ the radiological activity at the initial time instant, is defined in Eq. (4).

$$Ac = \{[\lambda \cdot T \cdot \rho \cdot V_g]/[(\lambda + R)V_r]\}\{1 - \exp[-(\lambda + R)t]\} + Ac_0 \exp[-(\lambda + R)t] \quad (4)$$

Health administrations from different countries and the World Health Organization set the maximum allowable concentration of radon in air between 100 and 400 $Bq \cdot m^{-3}$.

The mass of radon and its radiological activity concentration, $Ac$ ($Bq \cdot m^{-3}$), within the building and without any ventilation ($R = 0$), even without a minimum infiltration, is calculated based on Eq. (3) and Eq. (4) and from the values set out in the Abbreviations. The balance between the radon atoms escaped from granite to the surrounding air and the decay radon atoms is reached approximately after a month of storage of the granite slabs, having an amount of 2714.7 pg of radon in the building, being its concentration 989 $Bq \cdot m^{-3}$. For a maximum permissible concentration of 300 $Bq \cdot m^{-3}$, due to the presence of the radon, it is reached in about 2 days.

Moreover, Eq. (4) provides information on the radiological activity of the air after a break in the activities of the processing plant. In such cases, with doors and windows completely closed, all connection with outdoor air is neglected, i.e. the ventilation rate is $R = 0$. As an example it is considered the case of the plant closed on weekends, from Friday at 18 h, when radiological activity is, for example, 100 Bq $m^{-3}$, until Monday at 8 h. From Eq. (4), with $R = 0$, it is deduced that $A_c$ after 62 h is 433 $Bq \cdot m^{-3}$. If, after work activities resumption on Monday, a reduction of concentration is required, the lapse of time until satisfactory levels are reached depends on the ventilation rate. Thus, a ventilation system that provides an air flow rate of $R = 2\ h^{-1}$ reduces the radiological activity from 433 to 99 $Bq \cdot m^{-3}$ in 44 min time.

In the case of forced ventilation, the required air flow rate to maintain radon concentration to 300 $Bq \cdot m^{-3}$ is derived from Eq. (5), which in turn is obtained from Eq. (4) after making the constant equal to 300, concentration value that is obtained after 6 days, approximately.

$$300 = [\lambda \cdot T \cdot \rho \cdot V_g]/[(\lambda + R)V_r] \quad (5)$$

Clearing $R$ in this equation, with the values set out in the Abbreviations, a ventilation rate of $R = 4.8223 \cdot 10^{-6}$ air changes per second, i.e. 0.0174 air changes per hour, is eventually obtained.

It should be noted that this ventilation flow, despite being very low, would be theoretically sufficient to maintain the controlled radiological activity to a set limit. However, such low flow rates imply low speed and, therefore, little turbulence and admixing, making it very difficult to comply with the assumption of perfect dilution.

### 2.5.2. *Spatial gradient concentration scenarios*

In the following scenarios, the relative position of the blocks of granite (sources of radon) and the ventilation/extraction as well as the flow rate of fresh air entering the room have a significant influence.

It has been assumed the storage of ten blocks of granite (5 m long, 2 m wide and 2 m high = 20 $m^3$) in the plant, placed 2 m apart.

The distributions of the material considered for the simulations are:

- Symmetrical position: the blocks of granite are placed symmetrically with respect to the other planes of symmetry of the plant (Fig. 1).
- Asymmetrical position: the same 10 blocks have been placed 2 m from one of the longitudinal sides and 2 m from the end of the workshop (Fig. 2).

#### 2.5.2.1. *Natural ventilation.*

In this scenario, it is assumed that the door and the roof opening are open and that the exterior air is still. The movement of air and radon respond exclusively to the dispersion forces (mainly) and gravitational forces (to a lesser extent due to the very low concentration of radon).

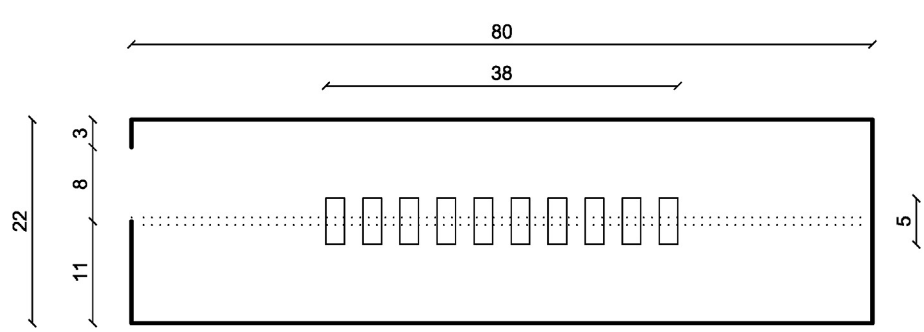


**Fig. 1.** Workshop floor. Symmetrical layout of the blocks of granite.

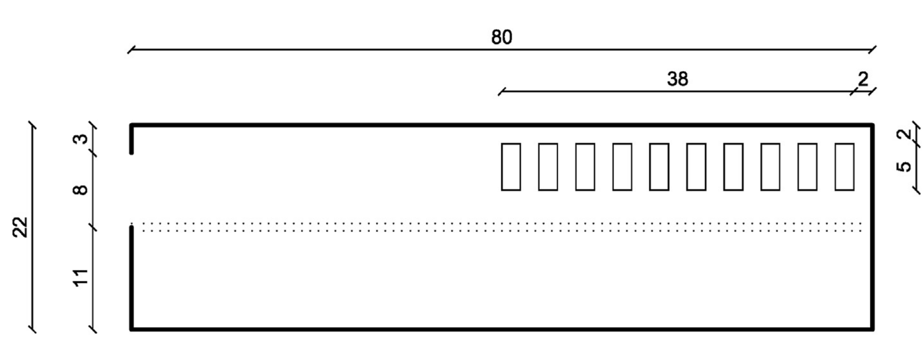


**Fig. 2.** Workshop floor. Asymmetrical layout of the blocks of granite.

*2.5.2.2. Forced ventilation.* Four ventilation air flow rates are considered: 80, 120, 160 and 200 $m^3/(m^2 \cdot h)$.

Both positions of the blocks of granite were simulated, symmetrical and asymmetrical, for natural and forced ventilation with the flow rates stated above.

## 3. Results and discussion

In the spatial gradients scenario, for each of the ten simulations, concentration of radon was expressed as $Bq \cdot m^{-3}$ on a theoretical horizontal plane situated at a height of 1.6 m from the floor. This height was chosen in order to measure the concentration of radon where the risk of inhalation by the workers is higher.

### 3.1. Natural ventilation

Figs. 3 and 4 show the results obtained for both the symmetrical and asymmetrical position of the blocks of granite.

Fig. 5 shows the concentration of radon over the control lines —shown as a black line in Figs. 3a and 4a— where the values of the X axis show the depth, taking a value equal to 0 at the access door and a value equal to 80 m at the end of the plant.

Figs. 3–5 clearly show the importance of the position of the blocks of granite. For an asymmetrical position, within almost half the length of the plant the radon concentration exceeds a value of 300 $Bq \cdot m^{-3}$ practically doubling the radiation permitted by legislation. Regarding the symmetrical position, the natural ventilation is sufficient to maintain the radiation within the legal limits.

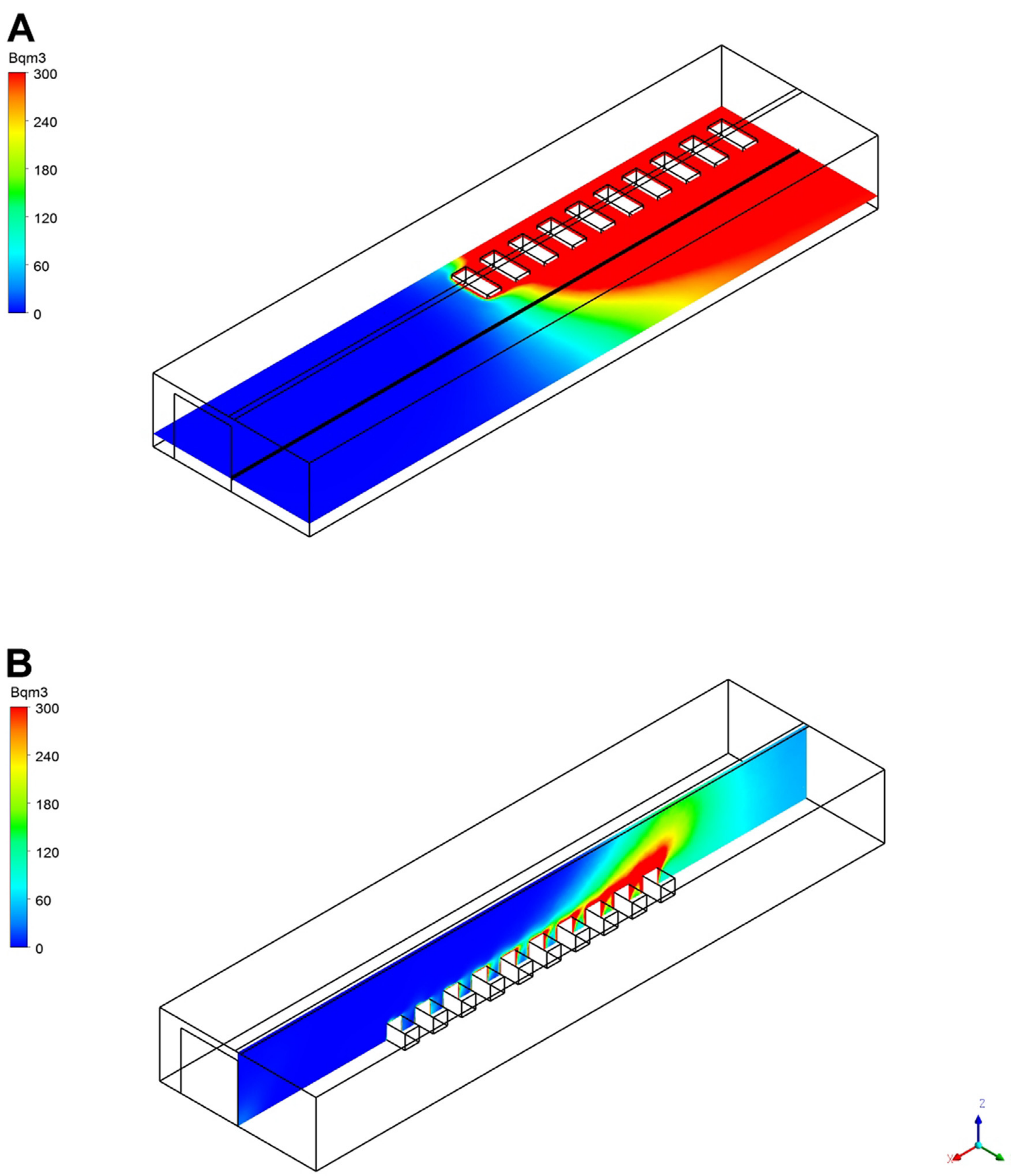


**Fig. 3.** Concentration of radon. Symmetrical position. Natural ventilation. a. Horizontal plane. b. Vertical plane.

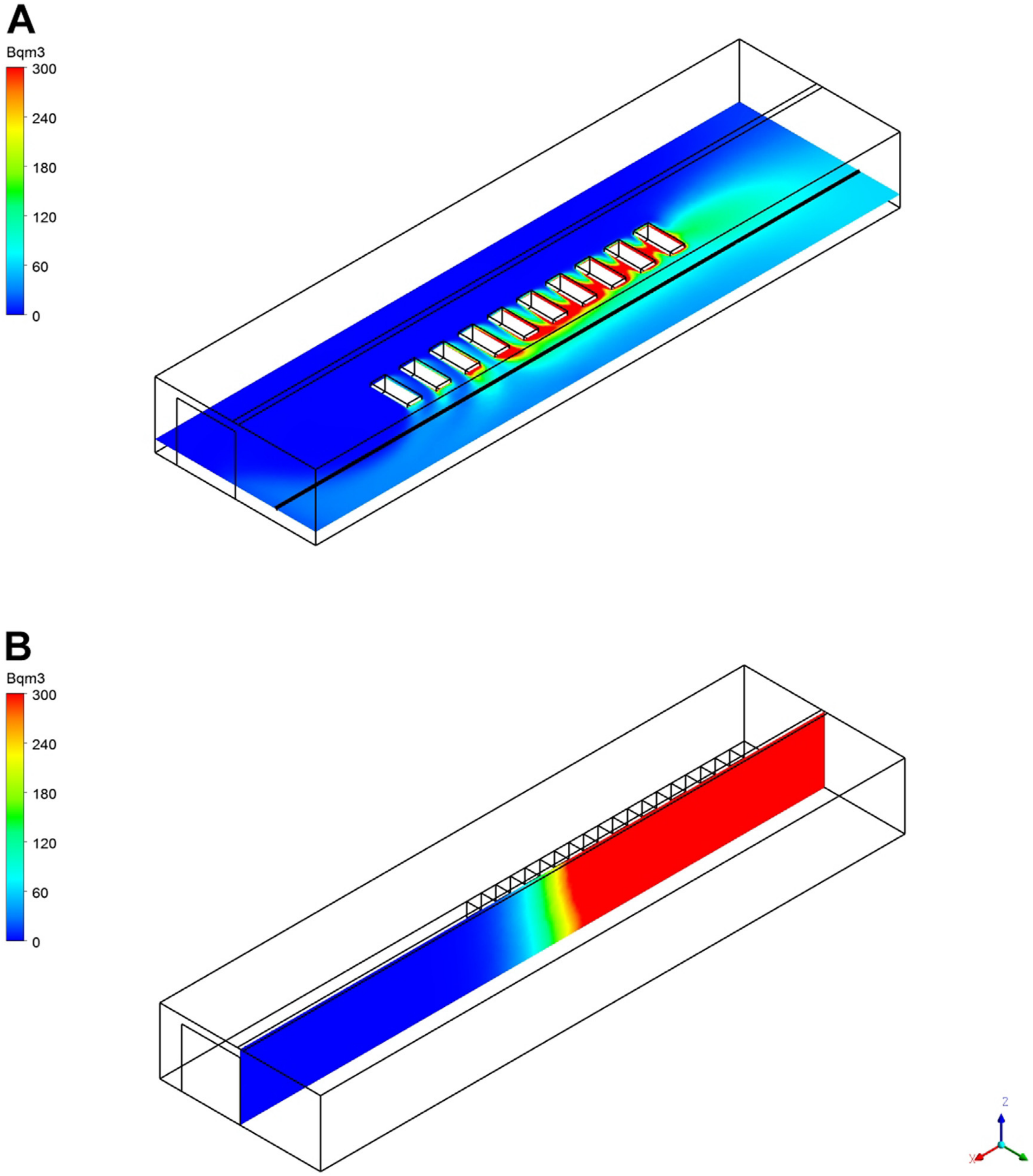


**Fig. 4.** Concentration of radon. Asymmetrical position. Natural ventilation. a. Horizontal plane. b. Vertical plane.

Since there is only natural ventilation and no mechanical extraction, it is of interest to foresee the way in which radon flows outside the plant. For the asymmetrical position of the blocks of granite, 99.9% of the radon escapes through the roof opening while the thousandth remaining part escapes through the door. For the symmetrical position (Fig. 6), 70% of the radon ($4.0 \cdot 10^{-15}$ g $s^{-1}$) escapes through the roof opening while the remaining 30% escapes through the door ($1.7 \cdot 10^{-15}$ g $s^{-1}$).

### 3.2. Forced ventilation

As mentioned previously, simulations were carried out with ventilation rates of 80, 120, 160 and 200 $m^3/(m^2 \cdot h)$.

#### 3.2.1. Asymmetrical position

Fig. 7 shows the concentration of radon for the simulated flows.

In general, the values found for this position in the four scenarios analysed compared to only natural ventilation for this same position (Fig. 5), are significantly lower. Specifically, the maximum values of radon concentration decrease approximately by half. Moreover, the maximum limit of 300 $Bq \cdot m^{-3}$ is only exceeded by 7.5% of the length of the plant (the last 6 m), while for natural ventilation the limit was exceeded from halfway along the plant. Finally, it can be observed that a ventilation rate of 200 $m^3/(m^2 \cdot h)$, enables the concentration of radon to be lowered to a value below the legal limit throughout all the working area of the plant.

#### 3.2.2. Symmetrical position

Fig. 8 shows the concentration of radon for the simulated flows.

The values found for the four scenarios analysed compared to only natural ventilation for this same position (Fig. 5), are significantly lower.

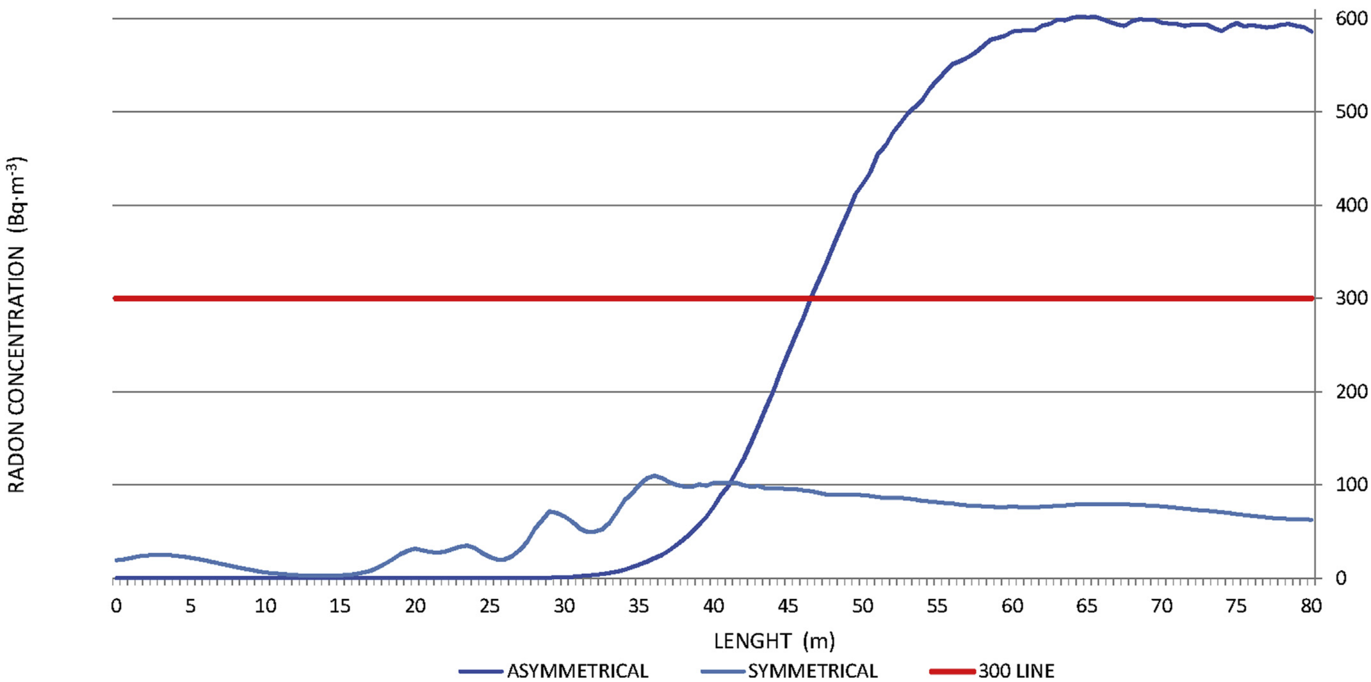


**Fig. 5.** Radon concentration over the control line. Symmetrical and asymmetrical position. Natural ventilation.

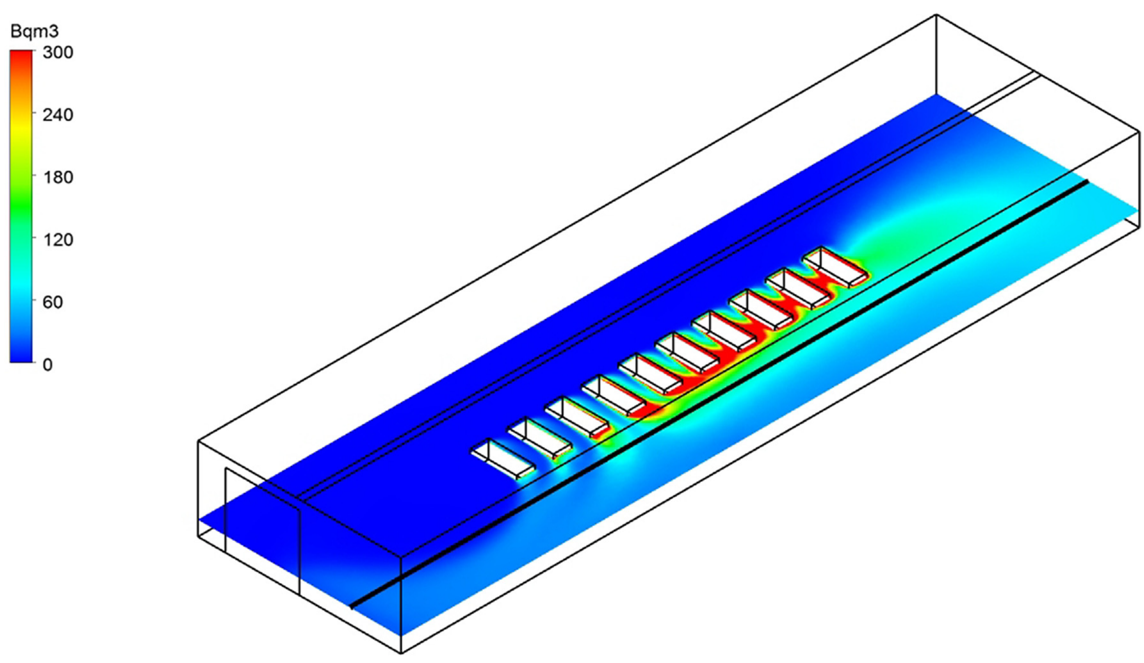


**Fig. 6.** Current lines. Symmetrical position. Natural ventilation.

The position of the blocks of granite is essential to the radiation distribution. The mean concentration of radon for the asymmetrical position is approximately between 3 and 4 times higher compared to the symmetrical position, regardless of the ventilation flow provided.

A symmetrical layout keeps the concentration of radon below the set limits. However, it can be seen that a 200 $m^3/(m^2 \cdot h)$ flow reduces the concentration of radon 10 times compared to the exclusive use of natural ventilation.

Table 3 shows the amount of radon within the plant, the mean concentration of radon assuming that such mass is in perfect dilution, the percentage volume of air in the plant that exceeds 100 and 300 $Bq \cdot m^{-3}$ as a function of the ventilation rate –0, 80, 120, 160 and 200 $m^3/(m^2 \cdot h)$– and of the position of the blocks of granite (A and S).

It may once again be stated that the layout of the blocks –the source of radon emission– is the key factor in the level of radioactive contamination.

An increase in the renewal flow means a reduction of the radon mass. This reduction is not proportional but exponential –an usual

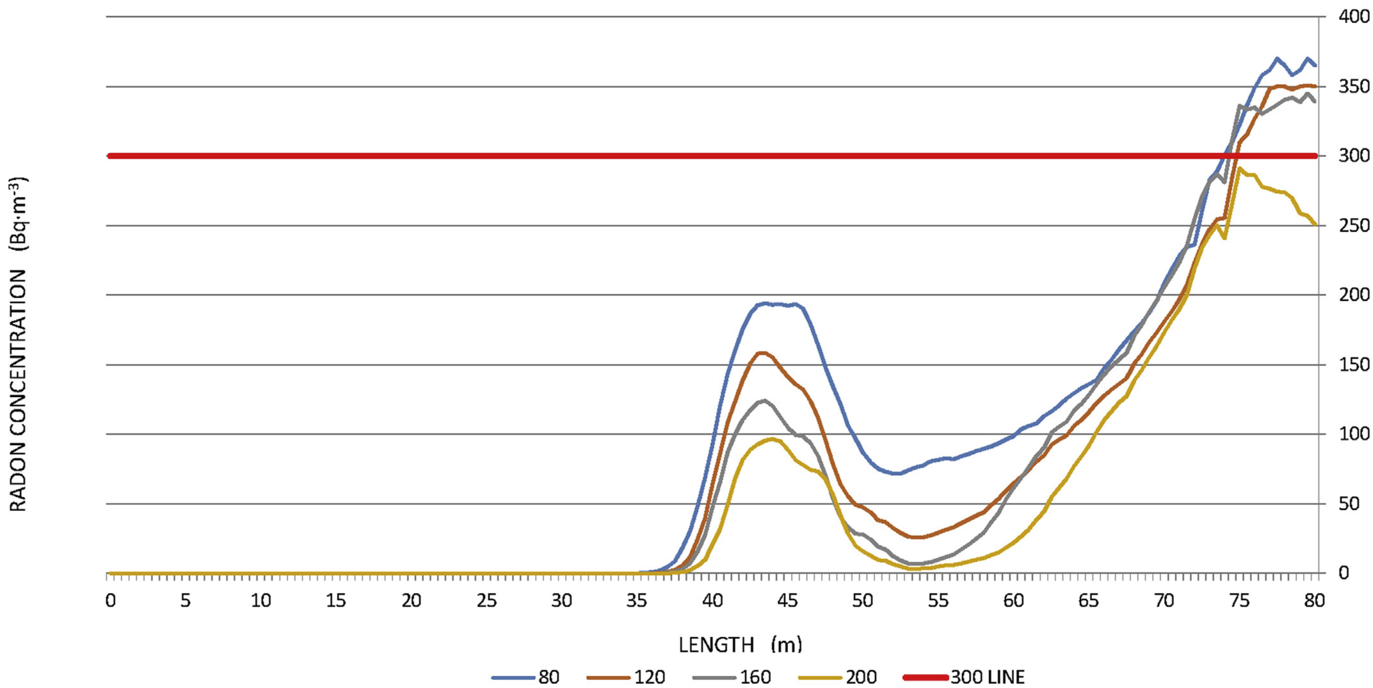


**Fig. 7.** Radon concentration over the control line. Asymmetrical position. Different ventilation flows.

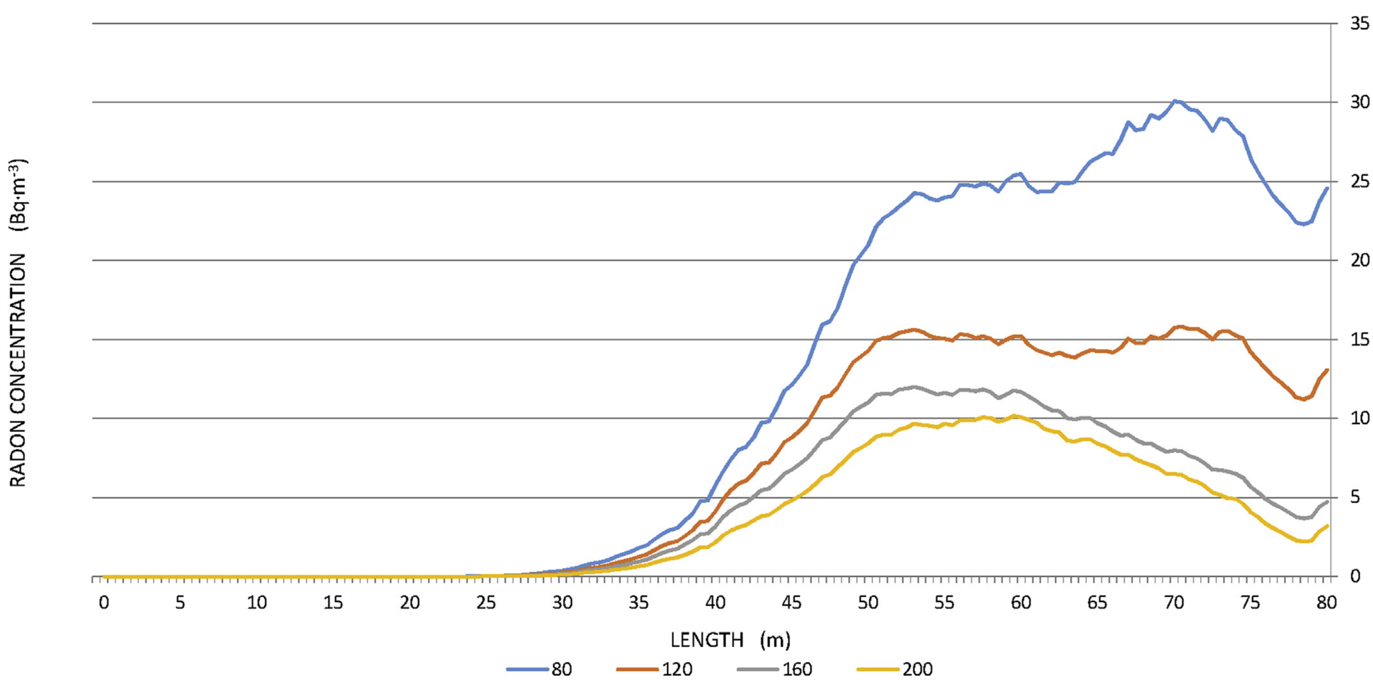


**Fig. 8.** Radon concentration over the control line. Symmetrical position. Different ventilation flows.

performance in dilution processes— asymptotic at zero or very low values as the renewal increases.

Rows in Table 3 indicate the following: first row refers to the total radon mass within the workshop. Second row shows the average radiological activity in the whole volume of the building, that is to say the concentration if the aforementioned mass of radon is completely diluted in the air volume. Third and fourth rows express the percentages of volume that exceed 100 and 300 $Bq \cdot m^{-3}$, respectively. For example, for the natural ventilation and symmetrical layout case, radon mass in the workshop is 830 pg, which implies an average concentration of 302 $Bq \cdot m^{-3}$. If dilution were perfect, 100% of the workshop volume should present concentration levels higher than 300 $Bq \cdot m^{-3}$. Nevertheless, the values obtained are 49% and 37%, respectively, results that reveal how the heterogeneity in the spatial distribution of radon prevails. Finally, values of 100 and 300 $Bq \cdot m^{-3}$ correspond to radon masses of 275 and 826 pg, respectively, if it is homogenously distributed.

In the section devoted to perfect dilution with air renewal, it is

**Table 3**
Radon mass, mean concentration of radon and fraction of volume contaminated as a function of the ventilation rate and the position of the blocks (A: asymmetrical S: symmetrical).

| | Ventilation rate $m^3/(m^2 \cdot h)$ | | | | | | | | | |
|---|---|---|---|---|---|---|---|---|---|---|
| | 0 | | 80 | | 120 | | 160 | | 200 | |
| | A | S | A | S | A | S | A | S | A | S |
| Radon Mass present (pg) | 830 | 79 | 140 | 61 | 124 | 41 | 99 | 26 | 56 | 20 |
| Mean concentration of radon ($Bq \cdot m^{-3}$) | 302 | 29 | 51 | 22 | 45 | 15 | 36 | 9 | 21 | 7 |
| % Volume concentration of radon >100$Bq \cdot m^{-3}$ | 49 | 8 | 13 | 7 | 11 | 5 | 9 | 3 | 5 | 3 |
| % Volume concentration of radon >300$Bq \cdot m^{-3}$ | 37 | 1 | 5 | 2 | 4 | 1 | 3 | 0 | 2 | 0 |

concluded that a flow of 271.5 $m^3\ h^{-1}$ keeps the concentration of radon at 300 $Bq \cdot m^{-3}$. For a door area of 64 $m^2$, a flow of 4.25 $m^3/(m^2 \cdot h)$ of renewed air, in a situation of perfect dilution, would be sufficient to maintain the concentration of radon at 300 $Bq \cdot m^{-3}$. Therefore, a good ventilation-extraction system should be able to dilute the radon to the maximum and prevent any zones of concentration.

In the symmetrical layout, it can be observed that a slightly higher percentage volume of air with concentration of radon is higher than 300 $Bq \cdot m^{-3}$ with an 80 $m^3/(m^2 \cdot h)$ ventilation rate, compared to the natural ventilation scenario. The amount of radon in the plant using natural ventilation is higher, as can be seen in Table 3, but the dispersion forces tend to dilute this greater amount of radon more effectively than a partially "short-circuited" current of air between the entrance and the exit.

It can also be seen that there are scenarios in which some zones of the plant pose a high risk to workers' health since they exceed 300 $Bq \cdot m^{-3}$. These zones coincide with the most distant points to the access doors at the end of the plant and can reach a third of the air volume within the plant. A ventilation-extraction system to prevent still air zones is necessary.

## 4. Conclusions

In general, metamorphic rocks like granite emit natural radiation since they contain all the radioisotopes of the natural radioactive chains of thorium $^{232}Th$, uranium $^{238}U$ and uranium $^{235}U$. These three chains contain a single gaseous radioactive element, radon. $^{222}Rn$ isotope is the only one that has a long enough life to be able to permeate through the rock into the surrounding air. Epidemiological studies have demonstrated a clear link between breathing in high concentrations of radon and the incidence of lung cancer. Therefore, radon is regarded as a significant contaminant that affects interior air quality.

In closed premises without ventilation where these rocks are handled, as in granite processing plants, radon concentrations that are incompatible with the working activity are quickly reached. In order to meet the health requirements set out in current legislation, these premises must be ventilated.

This research shows how to minimise the concentration of radon in a processing plant depending on how the blocks of granite are positioned and on the ventilation-extraction rate. The concentration increases significantly with an asymmetrical layout of the blocks. Regrettably, this layout is the most usual one, since there is a tendency to place the heavy material at both sides of the plant, leaving the central area clear for the transit of people and machinery.

A good radioactive decontamination system must tend towards a perfect dilution of the radon using air renewal and prevent any zones with still air, recirculation and any concentration of radon.

In essence, radon and air mixing is, as far as its chemical and physical properties are concerned, air with so low a percentage of radon that it does not affect either its aerodynamics or its chemical properties, although it certainly does with respect to its radiological properties. Thus, a CFD study of a radon-air mixture is essentially a CFD study of air, in which a small amount of atoms of radon is dragged.

## References


Agarwal, T.K., Joshi, M., Sahoo, B.K., Kanse, S.D., Sapra, B.K., 2016. Effect of 220Rn gas concentration distribution on its transmission from a delay chamber: evolving a CFD-based uniformity index. Radiat. Prot. Dosim. 168, 546–552.

Agarwal, T.K., Sahoo, B.K., Gaware, J.J., Joshi, M., Sapra, B.K., 2014. CFD based simulation of thoron (220Rn) concentration in a delay chamber for mitigation application. J. Environ. Radioact. 136, 16–21.

Akbari, K., Mahmoudi, J., Ghanbari, M., 2013. Influence of indoor air conditions on radon concentration in a detached house. J. Environ. Radioact. 116, 166–173.

Andersen, C.E., 2001. Numerical modelling of radon-222 entry into houses: an outline of techniques and results. Sci. Total Environ. 272, 33–42.

ATSDR, 1990. Toxicological Profile for Silver. U.S. Department of Health and Human Services. Public Health Service, Agency for Toxic Substances and Disease Registry, Atlanta.

BEIR, 1999. Report on the Committee on Biological Effects of Ionizing Radiation, Health Effects of Exposure to Radon, Biological Effects of Ionizing Radiation. National Research Council, National Academy Press, Washington DC.

Castren, O., Voutilainen, A., Winqvist, K., Mäkeläinen, I., 1985. Studies of high indoor radon areas in Finland. Sci. Total Environ. 45, 311–318.

Cavallo, A., Gadsby, K., Reddy, T.A., 1996. Comparison of natural and forced ventilation for radon mitigation in houses. Environ. Int. 22, 1073–1078.

Chao, C.Y.H., Tung, T.C.W., Chan, D.W.T., Burnett, J., 1997a. Determination of radon emanation and back diffusion characteristics of building materials in small chamber tests. Build. Environ 32, 355–362.

Chao, C.Y.H., Tung, T.C.W., Burnett, J., 1997b. Influence of ventilation on indoor radon level. Build. Environ 32, 527–534.

Chauhan, N., Chauhan, R.P., Joshi, M., Agarwal, T.K., Aggarwal, P., Sahoo, B.K., 2014. Study of indoor radon distribution using measurements and CFD modeling. J. Environ. Radioact. 136, 105–111.

Chen, J., Rahman, N.M., Atiya, I.A., 2010. Radon exhalation from building materials for decorative use. J. Environ. Radioact. 101, 317–322.

El-Hussein, A., 2005. A study on natural radiation exposure in different realistic living rooms. J. Environ. Radioact. 79, 355–367.

European Commission, 2001. Commission Recommendation of 20 December 2001 on the protection of the public against exposure to radon in drinking water supplies. Off. J. L 344, 85–88.

European Commission, 1999a. Radiation Protection 107: Establishment of Reference Levels for Regulatory Control of Workplaces where Materials Are Processed Which Contain Enhanced Levels of Naturally-occurring Radionuclides. Office for Official Publications of the European Communities, Luxembourg.

European Commission, 1999b. Radiation Protection 112: Radiological Protection Principles Concerning the Natural Radioactivity of Building Materials. Office for Official Publications of the European Communities, Luxembourg.

European Commission, 1997. Radiation Protection 88 : Recommendations for the Implementation of Title VII of the European Basic Safety Standards Directive (BSS) Concerning Significant Increase in Exposure Due to Natural Radiation Sources. Office for Official Publications of the European Communities, Luxembourg.

Ferrero, A., 2013. Caracterización radiológica de la episienita "Rojo Sayago". Salamanca University, Salamanca.

Gil-Lopez, T., Castejon-Navas, J., Galvez-Huerta, M.A., O'Donohoe, P.G., 2014. Energetic, environmental and economic analysis of climatic separation by means of air curtains in cold storage rooms. Energy Build 74, 8–16.

Gil-Lopez, T., Galvez-Huerta, M.A., Castejón-Navas, J., Gomez-Garcia, V., 2013a. A first approach to the problem of settling the ventilation rate that minimizes the predicted percentage of dissatisfied: application to a clean room. Adv. Sci. Lett. 19, 2823–2830.

Gil-Lopez, T., Castejon-Navas, J., Galvez-Huerta, M.A., Gomez-Garcia, V., 2013b. Predicted percentage of dissatisfied and air age relationship in ventilation

systems: application to a laboratory. HVAC&R Res. 19, 76–86.
Higgy, R.H., El-Tahawy, M.S., Abdel-Fattah, A.T., Al-Akabawy, U.A., 2000. Radionuclide content of building materials and associated gamma dose rates in Egyptian dwelling. J. Environ. Radioact. 50, 253–261.
IAEA, 2006. Assessing the Need for Radiation Protection Measures in Work Involving Minerals and Raw Materials, Safety Reports Series 49. International Atomic Energy Agency, Vienna.
IAEA, 2003. Radiation Protection against Radon in Workplaces Other than Mines, Safety Reports Series No. 33. International Atomic Energy Agency, Vienna.
ICRP, 2009. International Commission on Radiological Protection Statement on Radon. ICRP Ref 00/902/09.
Jelle, B.P., Noreng, K., Erichsen, T.H., Strand, T., 2011. Implementation of radon barriers, model development and calculation of radon concentration in indoor air. J. Build. Phys. 34, 195–222.
Loureiro, C.O., 1987. Simulation of the Steady-state Transport of Radon from Soil into Houses with Basement under Constant Negative Pressure, s.L, Report No. LBL-24378. Lawrence Berkeley Laboratory, Berkeley, CA.
NCRP, 1997. Measurement of Radon and Radon Daughters in Air. National Council for Radiation Protection and Measurement, Maryland. NCRP Report No. 97.
RD 1439, 2010. Reglamento sobre protección sanitaria contra radiaciones ionizantes, aprobado por Real Decreto 783/2001, Boletín Oficial del Estado 279. Spanish Government.
Righi, S., Bruzzi, L., 2006. Natural radioactivity and radon exhalation in building materials used in Italian dwellings. J. Environ. Radioact. 88, 158–170.
Sakoda, A., Ishimori, Y., Yamaoka, K., 2011. A comprehensive review of radon emanation measurements for mineral, rock, soil, mill tailing and fly ash. Appl. Radiat. Isotopes 69, 1422–1435.
Stoulos, S., Manolopoulou, M., Papastefanou, C., 2003. Assessment of natural radiation exposure and radon exhalation from building materials in Greece. J. Environ. Radioact. 69, 225–240.
Taylor, S.R., McLennan, S.M., 1985. The Continental Crust: its Composition and Evolution. Blackwell Scientific Publication, Oxford.
U.S. EPA, 2003. Assessment of Risks from Radon in Homes. Office of Radiation and Indoor Air, U.S. Environmental Protection Agency, Washington, DC.
UNSCEAR, 2006. Report to the general assembly. In: Scientific, Ann. E: Sources-to-effects Assessment for Radon in Homes and Workplaces, vol. II. United Nations Scientific Committee on the Effects of Atomic Radiation, New York.
UNSCEAR, 2000a. Exposures of Workers and the Public from Various Sources of Radiation. Report A/AC.82/-644. United Nations Scientific Committee on the Effects of Atomic Radiation, New York.
UNSCEAR, 2000b. Effects and Risk of Ionizing Radiation, Report to the General Assembly of the United Nations. United Nations Scientific Committee on the Effects of Atomic Radiation, New York.
Urosevic, V., Nikezic, D., Vulovic, S., 2008. A theoretical approach to indoor radon and thoron distribution. J. Environ. Radioact. 99, 1829–1833.
Wang, F., Ward, I.C., 2002. Radon entry, migration and reduction in houses with cellars. J. Build. Environ. 37, 1153–1165.
Wang, F., Ward, I.C., 2000. The development of a radon entry model for a house with a cellar. J. Build. Environ. 35, 615–631.
Wang, F., Ward, I.C., 1997. Modelling multiple radon entry and transport in a domestic dwelling. Build. Environ. 32, 341–350.
WHO, 2009. Handbook of indoor radon: a public health perspective. In: ShannounHZa (Ed.), Library Cataloguing. World Health Organization, Geneva.
WHO, 2007. International Radon Project Survey on Radon Guidelines, Programmes and Activities. World Health Organization, Geneva.
With, G.de, Jong, P.de, 2011. CFD modeling of thoron and thoron progeny in the indoor environment. Radiat. Prot. Dosim. 145, 138–144.
Zhuo, W., Iida, T., Morizumi, J., Aoyagi, T., Takahashi, I., 2001. Simulation of the concentrations and distributions of indoor radon and thoron. Radiat. Prot. Dosim. 93, 357–368.